# Effects of the boundary layer control methods on stability and separation point

Mihai-Vladut HOTHAZIE[1], Sterian DANAILA*,[1]

*Corresponding author
[1]University POLITEHNICA of Bucharest, Faculty of Aerospace Engineering,
Str. Polizu 1, Bucharest, Romania, 011061,
vlad.hothazie@gmail.com, sterian.danaila@upb.ro*

DOI: 10.13111/2066-8201.2021.13.1.8

*Received: 15 September 2020/ Accepted: 27 November 2020/ Published: March 2021*


***Abstract:*** *This paper concerns the benefits of the active boundary layer control methods. The main focus was studying the effectiveness of suction control for a laminar flow over an airfoil. However, injection normal to or along the wall was also approached using two numerical methods. For different values and distributions of the velocity control magnitude, a systematic comparison was done. Having the results of the laminar flow, a linear stability analysis based on the small disturbance theory was carried out obtaining both the neutral stability curves and the transition point. In the end, for each case, results were presented with the corresponding observations. Additionally, a study on the dependency of the separation point with respect to the injection velocity magnitude was done.*

***Key Words:*** *control, suction, injection, boundary-layer, separation, transition, stability*

## 1. INTRODUCTION

Numerous methods of improving the aerodynamic performance of an aircraft have been tested and validated. Nowadays, a great deal of research has been conducted in active boundary layer controls. Minimizing the boundary layer thickness with continuous suction or injection reduces the skin-friction drag considerably due to the increase of the laminar flow region [5]. The purpose of this paper is to study both the effectiveness of such methods and the influence on the transition point from laminar to turbulent flow.

A systematic methodology is presented starting with the governing equations of the laminar boundary layer. After that, solutions are obtained using two numerical methods. Starting with Cebeci-Smith's method, a Falkner-Skan transformation is done. The resulting third-order differential equation is then rewritten using Keller's box method as a system of first-order equations. After that, the system is linearized using Newton's method. This procedure yields a tridiagonal matrix-vector system which is solved using the block-elimination method. The second approach for solving the boundary layer equation is to rewrite them in a discrete form. An explicit formulation is used, and a stability analysis of the method is done using the circuit analogy method of Karplus.

Having the solutions of the laminar flow, a transition prediction is done using the semi-empirical $e^n$ method based on the small-disturbance theory. Finally, results are presented with a comparison between the two models, and the corresponding observations and conclusions are drawn.

## 2. METHODOLOGY

One method that proved to be efficient and reliable in increasing the high lift performance of an airfoil is the active boundary layer control with suction and fluid injection normal to or along the wall. The main objective of this method is to increase the area of the laminar flow by delaying the transition point with the positive effect of minimizing the friction drag. Starting with the governing equations and their corresponding boundary conditions, a numerical solution is obtained using both Cebeci-Smith's method [1] and an explicit method [2]. After that, a linear stability analysis is done using $e^n$ method to predict the transition point.

### 2.1 Laminar boundary-layer equations

The boundary layer region is represented by a thin layer over the surface where large velocity gradients occur. Thus, the effect of the viscous forces within the fluid cannot be neglected. Starting with a generally steady, two-dimensional, incompressible flow described by Navier-Stokes equations, a number of assumptions are made [6].

The first one states that the existence of the boundary layer theory is possible only for Reynolds numbers above a certain value, in aerodynamics $Re \geq 10^4$. The second one assumes that the boundary layer thickness is very small compared to the dimensions of the body of which it flows. This yields to a neglection of the body curvature, meaning that for a small particle flowing within the boundary layer region the effects of the centrifugal forces are insignificant. Although the boundary layer is very thin, a physical interpretation of its thickness is not possible. Thus, a theoretical thickness is introduced as being at the point where the velocity reaches 99% of the outer region. After all these assumptions the governing equations of the boundary layer become:

$$\begin{gathered} \frac{\partial u}{\partial x}+\frac{\partial v}{\partial y}=0 \\ u\frac{\partial u}{\partial x}+v\frac{\partial u}{\partial y}=U_e\frac{dU_e}{dx}+\nu\frac{\partial^2 u}{\partial y^2} \end{gathered} \tag{1}$$

with the corresponding boundary conditions:

$$\begin{gathered} y=0 \Rightarrow u=v=0 \\ y=\delta \Rightarrow u=U_e \end{gathered} \tag{2}$$

Having these equations, a Falkner-Skan transformation is done in which a transformed boundary layer thickness is introduced:

$$\eta = y\sqrt{\frac{U_e}{\nu x}} \tag{3}$$

together with a dimensional stream function:

$$f(x,\eta)=\frac{\psi(x,y)}{\sqrt{u_e \nu x}} \tag{4}$$

This transformation yields to a third-order differential equation in η:

$$(bf'')'+\frac{m+1}{2}ff''+m[1-(f')^2]=x\left(f'\frac{\partial f'}{\partial x}-f''\frac{\partial f}{\partial x}\right) \tag{5}$$

with the corresponding transformed boundary conditions:

$$\begin{aligned} \eta = 0 \ \Rightarrow \quad & \begin{cases} f = f_w = -\dfrac{1}{\sqrt{u_e \nu x}} \displaystyle\int_0^x v_w dx, \\ f' = 0 \end{cases} \\ \eta = \eta_e \Rightarrow \quad & f' = 1 \end{aligned} \tag{6}$$

### 2.2 Numerical solution using Cebeci-Smith's method

To solve eqs. (5) and (6) we use Keller's box method [3], in which we rewrite them as a system of first-order equations. Thus, two variables are introduced as follows:

$$u = f', \quad v = u' \tag{7}$$

Doing so, the equations become:

$$\begin{aligned} (bv)' + \frac{m+1}{2} fv + m(1-u^2) &= x\left(u\frac{\partial u}{\partial x} - v\frac{\partial f}{\partial x}\right) \\ \eta = 0 \ \Rightarrow \quad & \begin{cases} u = 0 \\ f = f_w(x) \end{cases} \\ \eta = \eta_e \Rightarrow \quad & u = 1 \end{aligned} \tag{8}$$

Now, the first order equations are approximated using central difference derivates and midpoint on an arbitrary rectangular net. This yields to following form of the system:

$$\begin{aligned} h_j^{-1}\left(b_j^n v_j^n - b_{j-1}^n v_{j-1}^n\right) + \alpha_1 (fv)_{j-1/2}^n - \alpha_2 (u^2)_{j-1/2}^n \\ + \alpha^n \left(v_{j-1/2}^{n-1} f_{j-1/2}^n - f_{j-1/2}^{n-1} v_{j-1/2}^n\right) = R_{j-1/2}^{n-1} \end{aligned} \tag{9}$$

where

$$\begin{aligned} R_{j-1/2}^{n-1} &= -L_{j-1/2}^{n-1} + \alpha^n \left[(fv)_{j-1/2}^{n-1} - (u^2)_{j-1/2}^{n-1}\right] - m^n \\ L_{j-1/2}^{n-1} &= \left\{h_j^{-1}\left(b_j v_j - b_{j-1} v_{j-1}\right) + \frac{m+1}{2}(fv)_{j-1/2} + m\left[1 - (u^2)_{j-1/2}\right]\right\}^{n-1} \end{aligned} \tag{10}$$

The boundary conditions are rewritten as follows:

$$f_0^n = f_w, \quad u_0^n = 0, \quad u_j^n = 1 \tag{11}$$

The nonlinear, implicit resulting system is linearized using Newton's method. Iterates are introduced for $f_j^{(\nu)}, u_j^{(\nu)}, v_j^{(\nu)}$ where $\nu = 0,1,2 \ldots$ We initialize the values of the variables at a $x$ station with the result from the previous station. For the next iterates a linear approximation is done:

$$\begin{aligned} f_j^{(\nu+1)} &= f_j^{(\nu)} + \delta f_j^{(\nu)} \\ u_j^{(\nu+1)} &= u_j^{(\nu)} + \delta u_j^{(\nu)} \\ v_j^{(\nu+1)} &= v_j^{(\nu+1)} + \delta v_j^{(\nu)} \end{aligned} \tag{12}$$

This procedure yield to a linear system with a block tridiagonal structure written in matrix vector form as follows:

$$A\vec{\delta} = \vec{r} \tag{13}$$

where $\vec{\delta}$ represent the unknowns, $\vec{r}$ the right-hand side of the system and $A$ a tridiagonal matrix. Using the block-elimination method, a solution of the system can be obtained efficiently.

### 2.3 Numerical solution using an explicit method

Another method for solving the boundary layer equations is approached using an explicit formulation**.**Using the parabolic momentum equation,an explicit downstream marching procedure is done to determine the $x$ component of the velocity. Similarly, from the auxiliary continuity equation, the $y$ component of the velocity is obtained.

The second derivative from the momentum equation, as well as the second term from the left-hand side, is written using a central difference for better accuracy. Also, the remaining terms are expressed similarly. The pressure gradient term is obtained using the inviscid solution. So, the momentum equation becomes:

$$u_{n+1,m} = Q_{n,m}\left(u_{n,m+1} + u_{n,m-1}\right) - \left(2Q_{n,m} - 1\right)u_{n,m} - \frac{U_e}{u_{n,m}}\left(U_{e_{n+1}} - U_{e_n}\right) - \frac{v_{n,m}}{u_{n,m}}\left(\frac{\Delta x}{\Delta y}\right)\left(\frac{u_{n,m+1} - u_{n,m-1}}{2}\right) \tag{14}$$

where

$$Q_{n,m} = \frac{\nu \Delta x}{u_{n,m}\Delta y^2} \tag{15}$$

It can be noted that the factor $Q_{n,m}$ depends on $u_{n,m}$ and not on $U_{e_n}$. This means that $Q_{n,m}$ is not constant across the layer at any $x$ station. Using this form of the equation the $x$ component of the velocity can be obtained. For the $y$ component, the auxiliary equation of the system is used. An expression similar to Keller's box method is applied, and the continuity equation becomes:

$$\frac{1}{2}\left[\frac{u_{n+1,m} - u_{n,m}}{\Delta x} + \frac{u_{n+1,m-1} - u_{n,m-1}}{\Delta x}\right] + \frac{v_{n+1,m} - v_{n+1,m-1}}{\Delta y} = 0 \tag{16}$$

Obtaining the components of the velocity, a stability analysis of the numerical scheme is done. Because of the nonlinearity of the original system, the von Neumann method can not be applied. So, a circuit analogy method of Karplus is used. This yields the following stability condition:

$$\Delta x \leq \frac{1}{2}\frac{u_{n,m}\Delta y^2}{\nu} \tag{17}$$

Using the above expression, it can be concluded that a variable step size along the surface is required for the explicit method.

Having a solution for the velocity components, both the displacement and momentum thickness can be obtained by integrating the velocity profiles.The wall shear-stress can be expressed as follows:

$$\tau_w = \mu\left(\frac{\partial u}{\partial y}\right)_{y=0} \approx \frac{\mu}{2\Delta y}\left(4u_{n,2} - u_{n,3}\right) \tag{18}$$

The code for this method was written in FORTRAN 90 and it was used in comparison to Cebeci-Smith's method for the injection/suction method of control normal to the wall. Also, a study of injection along the wall was done using this method with acceptable results.

### 2.4 Stability analysis

Having the solutions of the laminar flow, a linear stability analysis is done using the $e^n$ method. This is based on the assumption that transition occurs only when a small disturbance introduced at a critical number is amplified by a factor of $e^n$. In our paper, the spacial amplification theory was approached.

Based on a small disturbance theory [4], the governing equation for the linear stability analysis was derived. Assuming that the instantaneous components of the flow $u, v, p$ are divided into a mean flow term, $\overline{u}, \overline{v}, \overline{p}$ and a fluctuating one, $u', v', p'$, neglecting the squares and products of the fluctuating terms and assuming that the mean flow velocity $\overline{u}$ is a function of $y$ only, a system of equations in dimensionless quantities is obtained:

$$\begin{gathered} \frac{\partial u^{'}}{\partial x}+\frac{\partial v^{'}}{\partial y}=0 \\ \frac{\partial u^{'}}{\partial t}+u\frac{\partial u^{'}}{\partial x}+v^{'}\frac{\partial u}{\partial y}=-\frac{\partial p^{'}}{\partial x}+\frac{1}{R}\left(\frac{\partial^2 u^{'}}{\partial x^2}+\frac{\partial^2 u^{'}}{\partial y^2}\right) \\ \frac{\partial v^{'}}{\partial t}+u\frac{\partial v^{'}}{\partial x}=-\frac{\partial p^{'}}{\partial y}+\frac{1}{R}\left(\frac{\partial^2 v^{'}}{\partial x^2}+\frac{\partial^2 v^{'}}{\partial y^2}\right) \end{gathered} \tag{19}$$

This system of equations describes how disturbances originating near the wall spread out through the boundary layer. To study the properties of these equations we represent a two-dimensional disturbance as follows:

$$q^{'}(x,y,t)=q(y)e^{i(\alpha x-\omega t)} \tag{20}$$

where $\alpha$ is a dimensionless number and $\omega$ is the frequency of the disturbance. Also expressing the velocity components such that:

$$u^{'}=\frac{\partial \psi}{\partial y}, \quad v^{'}=\frac{\partial \psi}{\partial x} \tag{21}$$

the momentum equation becomes:

$$\frac{\partial}{\partial t}\nabla^2\psi+u\frac{\partial}{\partial x}(\nabla^2\psi)-\frac{\partial \psi}{\partial x}\frac{d^2u}{dy^2}=\frac{1}{R}\nabla^4\psi \tag{22}$$

Expressing the disturbance stream function as:

$$\psi=\phi(y)e^{i(\alpha x-\omega t)} \tag{23}$$

eqn. (22) becomes a fourth order differential equation for the amplitude $\phi(y)$, known as the Orr-Sommerfeld equation:

$$\phi^{iv}-2\alpha^2\phi^{''}+\alpha^4\phi=iR(\alpha u-\omega)\left(\phi^{''}-\alpha^2\phi\right)-iR\alpha u^{''}\phi \tag{24}$$

The solution of the equation is obtained using the spatial amplification theory where $\omega$ is realand $\alpha$ a complex number. The eigenvalues of the Orr-Sommerfeld equation are represented in $(\alpha, R)$ or $(\omega, R)$ diagrams. The value where $\alpha_i = 0$ represents the neutral stability curve separating the stable from the unstable region. To calculate the transition point, the amplification rate $-\alpha_i$ is calculated as a function of $R$ for dimensional frequencies $\omega^*$. After that, the variation of the integrated amplificated factor rate is derived using:

$$n = -\int_{x_0}^{x} \alpha_i dx \tag{25}$$

### 2.5 Numerical solution of the Orr-Sommerfeld equation

The numerical solution is similar to the solution of the boundary layer equations obtained using Cebeci-Smith's method. Applying Keller's box method, the Orr-Sommerfeld equation and its corresponding boundary condition are reduced to a first order system of equations:

$$\begin{aligned} \phi' &= f \\ f' &= s + \xi_1^2 \phi \\ s' &= g \\ g' &= \xi_1^2 s - \xi_3 \phi \end{aligned} \tag{26}$$

After that the system of equations is rewritten in a form of a tridiagonal matrix-vector form as follows:

$$A\vec{\vec{\delta}} = \vec{\vec{r}} \tag{27}$$

where $\vec{\vec{\delta}}$ represents the unknowns. We note that the system derived depends only on four parameters:

$$\vec{\vec{\delta}} = \vec{\vec{\delta}}(\alpha, \beta, \omega, R) \tag{28}$$

Because $\alpha$ and $\beta$ are complex numbers and $\omega$ is real, the solution depends on six scalars. Fixing four of these, the remaining ones can be calculated such that the boundary conditions are satisfied. This corresponds to an eigenvalue problem that is solved using an eigenvalue procedure described in Tuncer-Cebeci [2].

## 3. RESULTS

Airfoils that are designed for laminar flow make use of large areas with a negative pressure gradient moving the transition point closer to the trailing edge. This can be further improved by using active boundary layer controls. In the following, a series of results obtained using the methods presented in the methodology chapter are presented based on three cases: suction control with a constant or linear variation of the surface mass transfer and a combination between injection or suction with the same variation. For a NACA 2412, the displacement thickness, $\delta^*$, the momentum thickness, $\theta^*$, and the skin friction coefficient, $C_f$, are represented. For different angles of attack, the effect of the control method on the separation point was analyzed.

**Suction/ injection normal to the wall**

In case of suction/injection normal to the wall the following input data were required:

| | | | |
|---|---|---|---|
| Reference velocity [m/s] | 10 | Total number of control points | 200 |
| Reference length [m] | 1 | Total number of normal grid points | 95 |
| Kinematic viscosity [$m^2/s$] | 2E-5 | Starting suction/injection point | Freely chosen |
| Reynolds number | 500000 | Ending suction/injection point | Freely chosen |

Note that both the control velocity magnitude and the length of the control region are dimensionless values.

Although a wide range of angles of attack was tested, the boundary layer parameters represented in this paper are only for the case of a $4^o$ angle of attack.

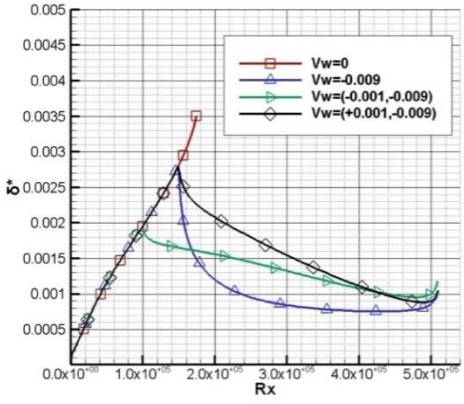


Figure 1. Displacement thickness obtained with Cebeci-Smith method

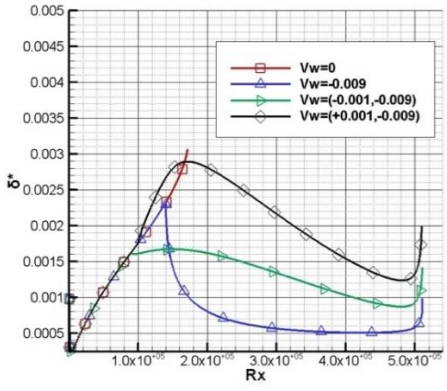


Figure 2. Displacement thickness obtained with the explicit method

The downstream development of the displacement thickness obtained with both methods for different suction and injection cases is shown in Figure 1 and Figure 2.

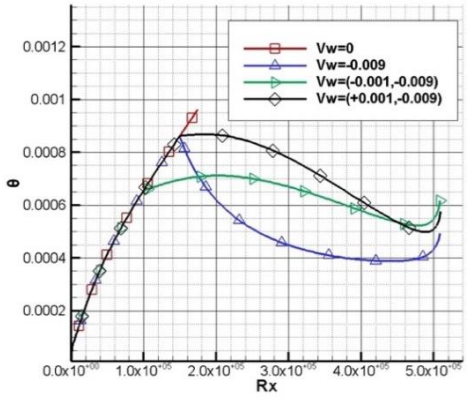


Figure 3. Momentum thickness obtained with Cebeci-Smith method

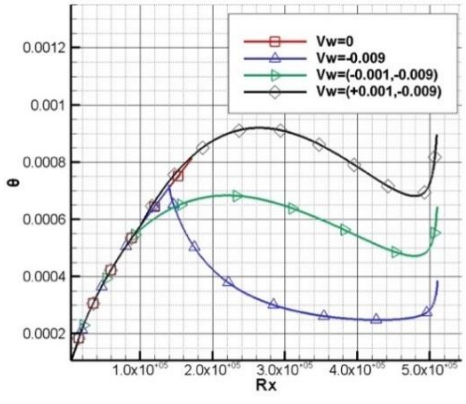


Figure 4. Momentum thickness obtained with the explicit method

In the case of suction, we note that in the control region, the displacement thickness is suppressed, and the separation point is shifted toward the trailing edge. On the other hand, injection promotes the displacement thickness to a higher value.

In Figure 3 and Figure 4 the variation of the momentum thickness with the local Reynolds number is portrayed.

In both cases, suction and injection, development is similar to the displacement thickness.

In the case of the explicit method with blowing, the values of the momentum thickness are higher than the ones from Cebeci-Smith's method. Also, in the case of constant suction, the overall values tend to be lower.

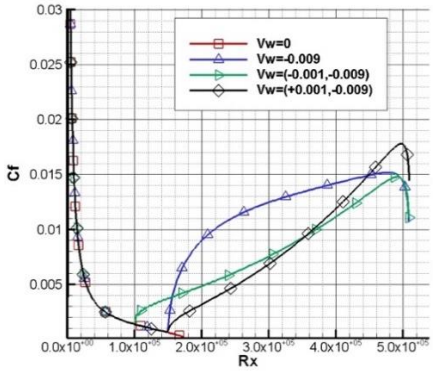


Figure 5. Skin friction coefficient obtained with Cebeci-Smith method

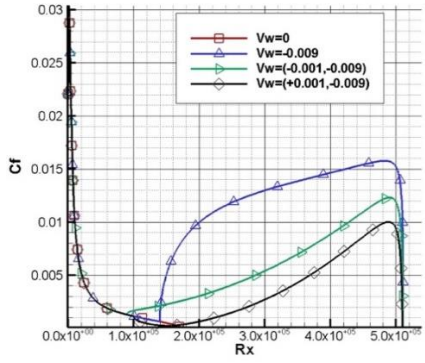


Figure 6. Skin friction coefficient obtained with the explicit method

Figure 5 and Figure 6 show the development of the skin friction coefficient with respect to the local Reynolds number. In the case of suction, the sharp rise of the skin friction coefficient comes from the high values of the velocity gradient due to the sudden decrease of the boundary layer. The explicit method gives a steeper slope because of the wall-shear stress approximation.

**Injection along the wall**

Results in case of injection along the wall were obtained using the explicit method. Having the same airfoil, NACA 2412, at the same angles of attack, three cases were tested. For the same angle of attack as in the previous case, a representation of the boundary layer parameters with respect to the local Reynolds number was plotted. Also, the following input data was necessary:

| | | | |
|---|---|---|---|
| Reference velocity [m/s] | 10 | Total number of control points | 200 |
| Reference length [m] | 1 | Total number of normal grid points | 100 |
| Kinematic viscosity [$m^2/s$] | 2E-5 | Total number of normal grid points in the initial section | 21 |
| Reynolds number | 500000 | Injection velocity magnitude | Freely chosen |

As in the previous case, the velocity magnitude is dimensionless. Also, instead of a control region, a point of injection is necessary.

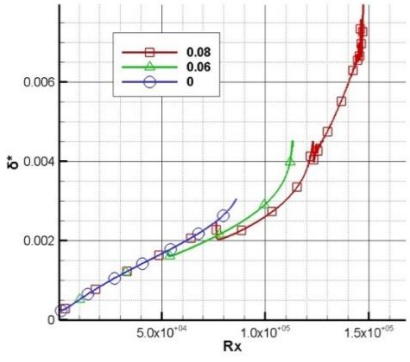


Figure 7. Displacement thickness obtained with the explicit method

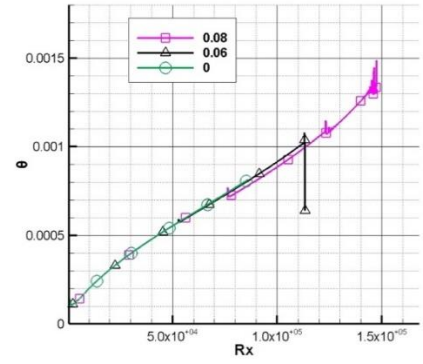


Figure 8. Momentum thickness obtained with the explicit method

The development of the displacement thickness, $\delta^*$, and the momentum thickness, $\theta$, along the wall is represented in Figure 7 and Figure 8. As expected in this case, both values have a steep increase past the region of the injection point. Also, numerical instabilities due to the nature of the scheme can be seen near the separation point.

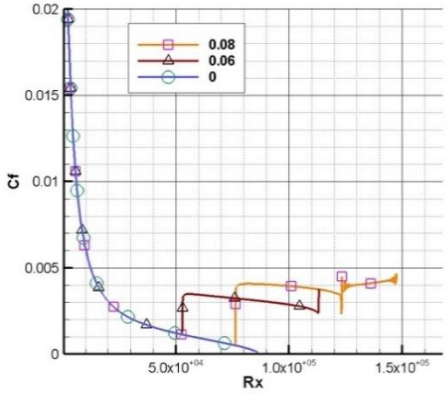


Figure 9. Skin friction coefficient obtained with the explicit method

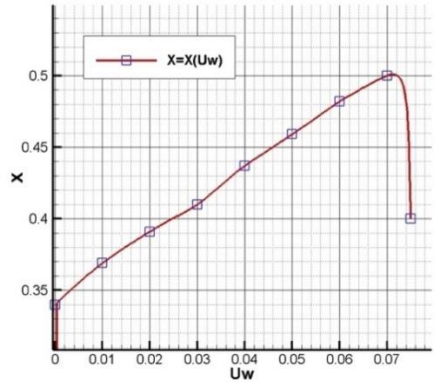


Figure 10. Dependency of the separation point with respect to the injection velocity magnitude

Figure 9 shows the variation of the skin friction coefficient with respect to the local Reynolds number. Past the injection point, a sharp rise occurs due to the high values of the $\frac{\partial u}{\partial y}$.The same instabilities near the separation point can be observed due to the wall-shear stress approximation.Figure 10 shows the variation of the separation point with respect to the injection velocity magnitude. It can be seen that past a certain value of the velocity magnitude, the effect of the control method is undesirable. Also, if the value is too small, the separation point remains unchanged.

**Stability analysis**

Flow transition was investigated for NACA 2412 using the $e^n$ method. The following input data was required for the stability analysis:

| | | | |
|---|---|---|---|
| Reference velocity [m/s] | 43 | Total number of control points | 200 |
| Reference length [m] | 1 | Total number of normal grid points | 100 |
| Kinematic viscosity [$m^2/s$] | 0. 00002 | Total number of tested frequencies | ≤5 |
| Reynolds number | 5000000 | The starting point of the stability analysis | Freely chosen |

As in the previous cases, the transition point was determined for a wide range of angles of attack as seen in the following table:

| RESULTS | | | | |
|---|---|---|---|---|
| AoA | Without control | | Suction control | |
| | Transition point | Separation point | Transition point | Separation point |
| $0^o$ | 0.342 | 0.96 | 0.449 | 1 |
| $2^o$ | 0.215 | 0.95 | 0.291 | 0.99 |
| $4^o$ | 0.107 | 0.93 | 0.138 | 0.98 |
| $6^o$ | 0.052 | 0.93 | 0.056 | 0.94 |

The following diagrams are represented only for the case of an $4^o$ angle of attack.

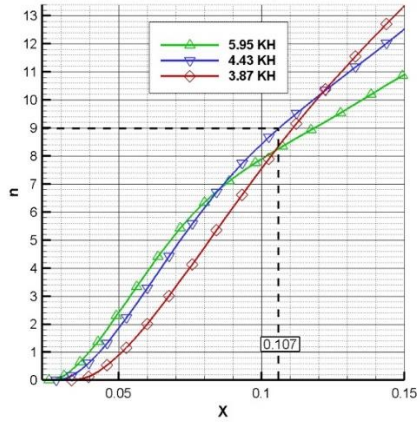


Figure 11. Transition prediction together with the integrated amplification rates (no control)

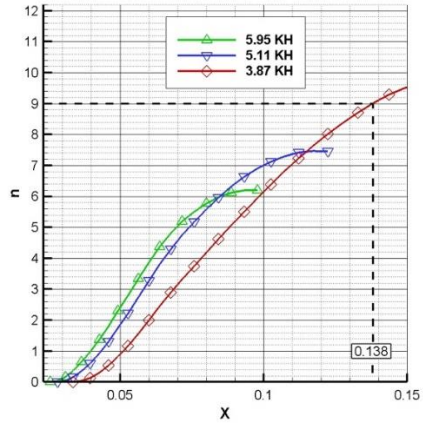


Figure 12. Transition prediction together with the integrated amplification rates ($V_w = -0.0009$)

Figure 11 and Figure 12 show the amplification factor $N$ for different frequencies. Also, the transition point is determined for $N = 9$. In the case of boundary layer control with suction, the transition point is delayed from 0.107 to 0.138.

The neutral stability curves of the amplification rate, $\alpha_i$, (Figure 14) and of the dimensional frequency, $\omega$, (Figure 13) represent the locus where $\alpha_i = 0$. Also, the instability region is defined by the area between the curves while the critical Reynolds number is the point where the first neutral stability point can occur. The beneficial effect of suction control can be seen due to the overall reduction of the region between the branches.

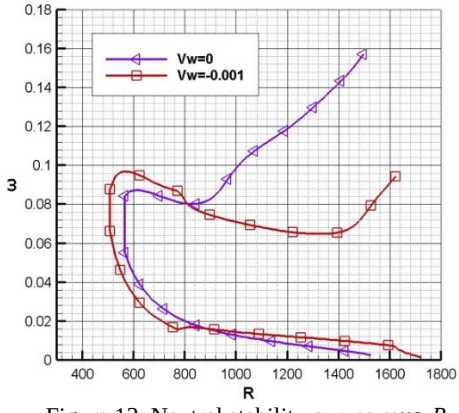


Figure 13. Neutral stability curves $\omega vs. R$

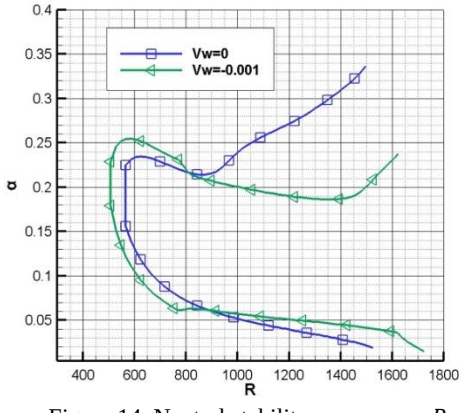


Figure 14. Neutral stability curves $\alpha vs. R$

On the other hand, a reduced critical Reynolds number in the suction case denotes a higher chance of instability.

## 4. CONCLUSIONS

This work proves that active boundary layer control can vastly improve the aerodynamic performance of an airfoil. In the case of the laminar flow, a very good agreement can be seen between the two methods. Although some differences can occur, the explicit method proves to be reliable and easier to implement. However, for more accurate results, Cebeci-Smith's method is recommended.

Both codes validate the following conclusions:

- Simulation over large areas of continuous suction/injection normal to the wall is well predicted;
- The influence of the control region is highly influencing the separation point;
- The suction velocity magnitude must not exceed a certain value, otherwise, the flow is separated prematurely.

In the case of injection along the wall, the velocity magnitude of the injected flow is one order higher than the suction/injection normal to the wall. Same as in the previous case, the values of the control velocity magnitude must be within a certain interval.

The stability analysis using the $e^n$ method proves to be reliable and consistent, although, errors may occur for angles of attack higher than $6^o$. Also, as expected, the transition point moves towards the leading edge with the increase of the angle of attack. The suction delays the transition point and the overall drag is reduced due to the increased area of laminar flow.

Although results are promising, a practical approach is rarely used because of the additional power required for the control system. Additionally, the overall trend in aviation is to lower complexity devices. However, with the recent advances in material and manufacturing, research in this field is highly encouraged due to the superior aerodynamic performances that can be achieved using these techniques.

## REFERENCES

[1] T. Cebeci, J. Cousteix, *Modeling and Computation of Boundary-Layer Flows*, Horizons Publishing Inc, 1999.
[2] J. Schetz, *Boundary Layer Analysis*, Prentice Hall, 1993.
[3] S.Dănăilă, C. Berbente, *Metode numerice în dinamica fluidelor*, Editura Academiei Române, 2003.
[4] S. Dănăilă, L. Moraru, *Tranzația laminar-turbulent*, Editura Printech, 2013.
[5] M.Fischer, R. Ash, *A general review of concepts for reducing skin friction, including recommendations for future studies*, Langley Research Center, 1974.
[6] H. Schlichting, *Boundary-Layer Theory*, Springer-Verlag Berlin Heidelberg, 2017.